Electromagnetic field quantization in amplifying dielectrics

Reza Matloob,[1,*] Rodney Loudon,[1] Maurizio Artoni,[1,2] Stephen M. Barnett,[2] and John Jeffers[2]
[1]*Department of Physics, University of Essex, Colchester CO4 3SQ, England*
[2] *Department of Physics and Applied Physics, University of Strathclyde, Glasgow G4 0NG, Scotland*
(Received 23 September 1996)

The electromagnetic field is quantized for normal transmission of incident waves through a parallel-sided dielectric slab. The dielectric material is dispersive and it acts as a linear amplifier over limited ranges of the frequency and as a linear attenuator at the remaining frequencies. The field operators derived for the three spatial regions within and on either side of the slab are shown to satisfy the canonical commutation relations. The noise fluxes emitted by the slab are evaluated and shown to satisfy the general requirements for the minimum noise associated with linear amplifiers and attenuators. The behavior of the amplifier gain profile on the approach to the lasing threshold of the slab is determined, but the results are restricted to the below-threshold state of the system. The spectra of the electric-field fluctuations are evaluated for the three spatial regions and for amplifying and attenuating frequencies. [S1050-2947(97)06402-0]

PACS number(s): 12.20.−m, 42.50.−p

I. INTRODUCTION

We have recently developed the quantum theory of the electromagnetic field in dielectric media that show both loss and dispersion [1,2], building on earlier work that is reviewed in these references (see also [3] for other work in the same area). Explicit results were given for the quantized field operators in propagation perpendicular to the interfaces of dielectric samples with the geometries of an infinite medium, a semi-infinite medium, and a parallel-sided slab. It was shown that the conjugate pairs of field operators correctly satisfy the required canonical commutation relations, and the spectra of the vacuum field fluctuations were evaluated and illustrated for the three sample geometries. The formalism has been used to evaluate the effects of propagation of an optical pulse through a dielectric slab on the pulse shape and photon statistics, including the nonclassical effects of photon antibunching and squeezing [4]. Similar quantization methods have also been applied to other geometries of dielectric material [5].

The aim of the present paper is to extend the field quantization to a dispersive dielectric that shows amplification over some ranges of the frequency and attenuation over the remaining ranges of frequency. We consider particularly a parallel-sided slab constructed from such dielectric material, again with electromagnetic wave propagation perpendicular to its surfaces. The infinite or semi-infinite sample geometries considered for the lossy dielectric lead to difficulties in the presence of gain, as any amplification inevitably produces infinite field fluctuations, and we do not consider them here. The slab geometry also gives rise to infinite path lengths in directions parallel to the surfaces and, although transverse effects are not explicitly treated, we assume a cross-sectional area sufficiently limited in its dimensions that only propagation perpendicular to the surfaces need be considered.

Despite the striking practical differences between media that show attenuation and those that show amplification over limited ranges of the frequency, their theoretical descriptions turn out to be remarkably similar. We can accordingly rely on slightly modified forms of many of the results given in [2], and this paper and its equations are identified by the abbreviation I. Of course, in agreement with the practical situation, the physical predictions of the amplifier theory, in terms for example of high-gain behavior, lasing threshold effects, and enhanced electric-field fluctuations, are quite different from those of attenuator theory. The similarities between their formal theories should not therefore obscure their very dissimilar physical natures. Brief details of our calculations have been given previously [6].

The general features of the dielectric function and the noise operators for media that show amplification and attenuation in different spectral ranges are introduced in Sec. II. The formal quantization of the electromagnetic field in the three spatial regions is performed in Sec. III. It is shown that the field operators satisfy the required canonical commutation relations provided that the magnitude of the round-trip gain inside the slab is less than unity, so that the lasing threshold is not achieved at any of the frequencies for which the dielectric behaves as an amplifier. The output noise fluxes and the transmission and reflection gains or losses of the slab are determined in Sec. IV, and it is shown that these satisfy general requirements derived for the minimum noise in amplifiers and attenuators. The behavior of the gain profile on the approach to the threshold for laser action is determined and shown to display the well-known phenomena of divergent peak gain and narrowing of the width of the gain spectrum. The spectra of the electric field fluctuations in the zero-temperature vacuum and at elevated temperatures are evaluated and illustrated for frequencies at which the medium shows amplification (negative effective temperature) and at which it shows attenuation (positive effective temperature). The main conclusions of the paper and its relation to previous work are summarized in Sec. V.

*Present address: Department of Physics, University of Kerman, Kerman, Iran.

II. DIELECTRIC PROPERTIES

In this section we define the geometrical arrangements of the slab and the electromagnetic fields to be quantized. We also consider the general properties of the dielectric functions that describe amplifying and attenuating media, and of the associated noise operators.

A. Dielectric function

The dielectric slab is taken to have a thickness $2l$, with the x coordinate perpendicular to its surfaces and the coordinate origin at its center. With free space on both sides of the slab, the system dielectric function is

$$\varepsilon(x,\omega)=\begin{cases}1 & \text{for} \quad x<-l \\ \varepsilon(\omega) & \text{for} \quad -l<x<l \\ 1 & \text{for} \quad l<x.\end{cases} \tag{2.1}$$

The electromagnetic properties of the medium are specified by its dielectric function $\varepsilon(\omega)$ at angular frequency ω, related to the complex refractive index $n(\omega)$ in the usual way

$$\varepsilon(\omega)=[n(\omega)]^2, \tag{2.2}$$

where the real refractive index $\eta(\omega)$ and extinction coefficient $\kappa(\omega)$ are defined by

$$n(\omega)=\eta(\omega)+i\kappa(\omega). \tag{2.3}$$

The dielectric function in an attenuating medium has well-known analytic properties [7], in particular that all of its poles lie in the lower half of the complex ω plane, in accordance with causality requirements. As a consequence, the above optical functions satisfy a range of dispersion, or Kramers-Kronig, relations and sum rules [8,9].

An amplifying medium is characterized by the existence of frequencies ω for which the extinction coefficient $\kappa(\omega)$ is negative and the loss is accordingly replaced by gain. The dielectric characteristics at such frequencies are calculated straightforwardly, using, for example, models of optically pumped media [10], and they can be described by the same functions as defined above. It is found that the dielectric function continues to have all of its poles in the lower half of the complex ω plane, with the difference that the signs of the residues are changed when an attenuating pole is replaced by an amplifying pole [11,12]. In general, the dielectric function of an amplifying medium has limited ranges of ω where $\kappa(\omega)$ is negative, while $\kappa(\omega)$ is positive or zero for all other frequencies. The optical functions of a pumped medium continue to satisfy similar dispersion relations and sum rules [12–14] to those for an entirely lossy dielectric. Furthermore, the dielectric function continues to conform to the limit

$$\varepsilon(\omega)\rightarrow 1 \quad \text{for} \quad \omega\rightarrow\infty \quad \text{in any manner}, \tag{2.4}$$

and the crossing relations

$$\varepsilon(-\omega)=\varepsilon^*(\omega), \quad n(-\omega)=n^*(\omega),$$

$$\eta(-\omega)=\eta(\omega), \quad \kappa(-\omega)=-\kappa(\omega) \tag{2.5}$$

continue to define the optical functions at negative frequencies.

A simple dielectric model is provided by the example of a system that has an upper level with population N_u and a lower level with population N_l, separated by energy $\hbar\omega_0$. The dielectric function for frequencies in the vicinity of the transition has the Lorentzian form

$$\varepsilon(\omega)=\varepsilon_b(\omega)-\frac{N_l-N_u}{N_l+N_u}\frac{\Sigma}{(\omega+\omega_0+i\gamma)(\omega-\omega_0+i\gamma)}, \tag{2.6}$$

where γ is a damping parameter, Σ denotes the strength of the resonance at ω_0 when all of the population is in one of the levels, and $\varepsilon_b(\omega)$ is a real background contribution to the dielectric function from all of the other resonances. The poles of the dielectric function always lie in the lower half plane at $\omega=\pm\omega_0-i\gamma$, while the residue of the more important pole at $\omega=\omega_0-i\gamma$ is negative for an attenuating resonance with normal populations, $N_l>N_u$, but positive for an amplifying resonance with inverted population, $N_l<N_u$.

As in I, we consider only electromagnetic waves that propagate perpendicular to the slab with their wave vectors parallel to the x axis and with their transverse electric and magnetic vector operators $\hat{E}(x,t)$ and $\hat{B}(x,t)$ parallel to the y and z axes, respectively. Thus with the usual decompositions of the operators into positive and negative frequency components and Fourier transform operators defined by

$$\hat{E}^+(x,t)=\frac{1}{\sqrt{2\pi}}\int_0^\infty d\omega\ \hat{E}^+(x,\omega)e^{-i\omega t}, \tag{2.7}$$

the electric- and magnetic-field operators are related to the vector potential operator by

$$\hat{E}^+(x,\omega)=i\omega\hat{A}^+(x,\omega), \quad \hat{B}^+(x,\omega)=\frac{\partial\hat{A}^+(x,\omega)}{\partial x}. \tag{2.8}$$

Substitution of these fields into Maxwell's equations produces an equation for the vector potential operator in the form

$$-\left(\frac{\partial^2}{\partial x^2}+\frac{\omega^2\varepsilon(x,\omega)}{c^2}\right)\hat{A}^+(x,\omega)=\mu_0\hat{j}(x,\omega), \tag{2.9}$$

where the transverse current operator $\hat{j}(x,\omega)$ plays the role of a Langevin force associated with the noise sources in the dielectric [2]. This operator vanishes in the absence of loss or gain, while in their presence it has the form

$$\hat{j}(x,\omega)=\theta(\kappa(\omega))\ \hat{j}^+(x,\omega)+\theta(-\kappa(\omega))\ \hat{j}^-(x,\omega), \tag{2.10}$$

where $\theta(Z)$ is the usual unit step function

$$\theta(Z)=\begin{cases}1 & \text{for} \quad Z>1\\ 0 & \text{for} \quad Z<1.\end{cases} \tag{2.11}$$

The replacement of the operator $\hat{j}^{+}$ for the attenuating medium by $\hat{j}^{-}$ for the amplifying medium is associated with the inversion of the noise oscillators in the latter (see [15,16]).

The solution of Eq. (2.9) for the vector potential operator is obtained by standard Green function methods in the form

$$\hat{A}^{+}(x,\omega)=S\int_{-\infty}^{\infty}dx'\,G(x,x',\omega)\hat{j}(x',\omega), \tag{2.12}$$

where S is an area of quantization in the y-z plane, and the Green function is determined by solution of

$$-\left(\frac{\partial^2}{\partial x^2}+\frac{\omega^2\varepsilon(x,\omega)}{c^2}\right)G(x,x',\omega)=\frac{\mu_0}{S}\delta(x-x'). \tag{2.13}$$

The Fourier transform Green function is the same as in I,

$$G(x,k,\omega)=\frac{1}{\sqrt{2\pi}}\int_{-\infty}^{\infty}dx'\,G(x,x',\omega)e^{ikx'}$$

$$=\frac{\mu_0}{\sqrt{2\pi}S}\,\frac{e^{ikx}}{k^2-[\omega^2\varepsilon(x,\omega)/c^2]}, \tag{2.14}$$

where $\varepsilon(x,\omega)$ is independent of x within each of the three spatial regions defined in Eq. (2.1).

B. Noise operators

The momentum conjugate to the vector potential in the Coulomb gauge is $-\varepsilon_0\hat{E}(x,t)$, and their equal-time commutator can be expressed in terms of the Green function as [5,17]

$$[\hat{A}(x,t),-\varepsilon_0\hat{E}(x',t)]=i\frac{2\varepsilon_0\hbar}{\pi}\int_0^{\infty}d\omega\;\omega\;\mathrm{Im}[G(x,x',\omega)]. \tag{2.15}$$

The commutator is required to reduce to the canonical form

$$[\hat{A}(x,t),-\varepsilon_0\hat{E}(x',t)]=(i\hbar/S)\delta(x-x'), \tag{2.16}$$

and this condition is used to establish the normalization of the Langevin noise operators. Thus, for noise that is uncorrelated at different positions and different frequencies, the result obtained in I (2.20) and in (4.38) of [17] is generalized to

$$[\hat{j}^{+}(x,\omega),\hat{j}^{-}(x',\omega')]=\{4\varepsilon_0\hbar\omega^2\eta(\omega)|\kappa(\omega)|/S\}\times\delta(x-x')\,\delta(\omega-\omega') \tag{2.17}$$

and it follows from the definition (2.10) of the generalized noise operator that

$$[\hat{j}(x,\omega),\hat{j}^{\dagger}(x',\omega')]=\{4\varepsilon_0\hbar\omega^2\eta(\omega)\kappa(\omega)/S\}\delta(x-x')\times\delta(\omega-\omega'). \tag{2.18}$$

We shall see in the Sec. III C that this normalization of the noise current commutator ensures compliance of the field operators with the canonical commutator (2.16). It is seen from Eqs. (2.17) and (2.18), respectively, that in regions of ω for which amplification occurs, $\kappa(\omega)$ sometimes appears as a positive magnitude and sometimes as a negative quantity.

Again similar to the derivations in I, it is convenient to use a normalized version $\hat{f}(x,\omega)$ of the noise current operator, defined by

$$\hat{f}(x,\omega)=\hat{j}^{+}(x,\omega)/\sqrt{4\varepsilon_0\hbar\omega^2\eta(\omega)|\kappa(\omega)|/S}, \tag{2.19}$$

and it is seen from Eq. (2.17) that this satisfies the simple boson commutation relation

$$[\hat{f}(x,\omega),\hat{f}^{\dagger}(x',\omega')]=\delta(x-x')\,\delta(\omega-\omega'). \tag{2.20}$$

The corresponding normalized version of Eq. (2.10) is given by

$$\hat{\varphi}(x,\omega)=\theta(\kappa(\omega))\hat{f}(x,\omega)+\theta(-\kappa(\omega))\hat{f}^{\dagger}(x,\omega), \tag{2.21}$$

and this new noise operator has a boson-type commutator

$$[\hat{\varphi}(x,\omega),\hat{\varphi}^{\dagger}(x',\omega')]=\mathrm{sgn}[\kappa(\omega)]\,\delta(x-x')\,\delta(\omega-\omega'). \tag{2.22}$$

The expectation values of these noise operators determine the amounts of noise that are added to optical signals that propagate through the attenuating or amplifying dielectric. The state of the dielectric slab at frequencies ω for which attenuation occurs is conveniently characterized by a positive frequency-dependent effective temperature $T\equiv T(\omega)$ and the noise operator expectation values are taken in the standard forms

$$\langle\hat{f}(x,\omega)\rangle=\langle\hat{f}^{\dagger}(x,\omega)\rangle=0 \tag{2.23}$$

and

$$\langle\hat{f}^{\dagger}(x,\omega)\hat{f}(x',\omega')\rangle=N(\omega,T)\,\delta(x-x')\,\delta(\omega-\omega'). \tag{2.24}$$

The population factor can be written in the equivalent forms

$$N(\omega,T)=\frac{1}{\exp(\hbar\omega/k_BT)-1}=\frac{N_u}{N_l-N_u}, \tag{2.25}$$

where N_u and N_l are the upper- and lower-level populations associated with the dielectric response at frequency ω, as used in the specimen two-level dielectric function (2.6), with $N_l>N_u$ for frequencies at which attenuation occurs. Very high temperatures correspond to saturation of the transition between the two levels, with $N_l=N_u$.

The corresponding results for an amplifying dielectric are obtained by taking a negative effective temperature, with use of the property

$$N(\omega,T)=N(\omega,-|T|)=-N(\omega,|T|)-1 \qquad \text{for} \quad T<0. \tag{2.26}$$

Thus the expectation value (2.23) is unchanged, but Eq. (2.24) is modified by the substitution of $N(\omega,|T|)$ for the population factor, which can be written in the equivalent forms

$$N(\omega,|T|)=\frac{1}{\exp(\hbar\omega/k_B|T|)-1}=\frac{N_l}{N_u-N_l}, \quad (2.27)$$

with $N_u>N_l$ for frequencies at which amplification occurs. The effective temperature $|T|=0$ corresponds to perfect inversion, with $N_l=0$, while very high temperatures $|T|\to\infty$ again correspond to saturation of the transition between the two levels, with $N_l=N_u$.

The noise operator defined by Eq. (2.21) is used in all subsequent calculations, and its expectation values determined by Eqs. (2.20), (2.23), (2.24), and (2.26) are

$$\langle\hat{\varphi}^\dagger(x,\omega)\hat{\varphi}(x',\omega')\rangle=\{\theta(\kappa(\omega))N(\omega,T)+\theta(-\kappa(\omega))[N(\omega,|T|)+1]\}\times\delta(x-x')\,\delta(\omega-\omega') \quad (2.28)$$

and

$$\langle\hat{\varphi}(x,\omega)\hat{\varphi}^\dagger(x',\omega')\rangle=\{\theta(\kappa(\omega))[N(\omega,T)+1]+\theta(-\kappa(\omega))N(\omega,|T|)\}\delta(x-x')\times\delta(\omega-\omega'), \quad (2.29)$$

and these are seen to be consistent with Eq. (2.22).

III. FIELD QUANTIZATION

The formal quantization of the electromagnetic fields in the slab and the free space regions on either side is performed in the present section. The methods are identical to those used in I, and many of the results are also the same. The account given below is therefore restricted to an outline of the procedure and presentation of those detailed results where the occurrence of amplifying behavior over some ranges of frequency produces changes from the results for a purely attenuating medium. The physical significances of the various results are discussed in Sec. IV.

The Green functions determined by solution of Eq. (2.13) are the same as for a purely attenuating dielectric and the results are given by I (5.2), (5.6), and (5.7). A particular integral solution for the vector potential operator is obtained by substitution of the appropriate Green function into Eq. (2.12). The complete solution also contains complementary function parts that correspond to free fields incident on the slab surfaces from the regions of free space to its left and right. The notation for the operators associated with the rightwards and leftwards parts of the fields in the three spatial regions is illustrated in Fig. 1. The operators for the incoming fields on the left and right of the slab have the free-space commutators

$$[\hat{a}_R(\omega),\hat{a}_R^\dagger(\omega')]=[\hat{b}_L(\omega),\hat{b}_L^\dagger(\omega')]=\delta(\omega-\omega'), \quad (3.1)$$

and the operators for the two kinds of incoming wave commute,

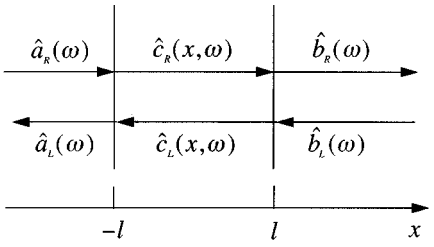

FIG. 1. Representation of the dielectric slab, showing the notation for the destruction operators used in the definitions of the vector potential operator.

$$[\hat{a}_R(\omega),\hat{b}_L^\dagger(\omega')]=0. \quad (3.2)$$

A. Exterior regions

Consider first the complete fields exterior to the slab. The field on the left can be written in the form

$$\hat{A}^+(x,t)=\int_0^\infty d\omega\left(\frac{\hbar}{4\pi\varepsilon_0 c\omega S}\right)^{1/2}[\hat{a}_R(\omega)e^{i\omega x/c}+\hat{a}_L(\omega)e^{-i\omega x/c}]e^{-i\omega t}, \quad x<-l, \quad (3.3)$$

where the operator for the leftward-propagating outgoing field is given by

$$\hat{a}_L(\omega)=R_S(\omega)\hat{a}_R(\omega)+T_S(\omega)\hat{b}_L(\omega)+\hat{F}_L(\omega), \quad (3.4)$$

similar to I (5.11). The outward-propagating noise operator is defined as

$$\hat{F}_L(\omega)=i\left(\frac{2\omega\eta(\omega)|\kappa(\omega)|}{c}\right)^{1/2}\times\int_{-l}^{l}dx'\left\{V(\omega)\exp\left(\frac{i\omega n(\omega)x'}{c}\right)+W(\omega)\exp\left(-\frac{i\omega n(\omega)x'}{c}\right)\right\}\hat{\varphi}(x',\omega). \quad (3.5)$$

The amplitude reflection and transmission coefficients for the slab are given by

$$R_S(\omega)=-\frac{n(\omega)^2-1}{D(\omega)}\exp\left(-\frac{2i\omega l}{c}\right)\times\left\{1-\exp\left(\frac{4i\omega n(\omega)l}{c}\right)\right\} \quad (3.6)$$

and

$$T_S(\omega)=\frac{4n(\omega)}{D(\omega)}\exp\left(\frac{2i\omega[n(\omega)-1]l}{c}\right). \quad (3.7)$$

The coefficients in the integrand of the noise operator are

$$V(\omega)=\frac{2[n(\omega)+1]}{D(\omega)}\exp\left(\frac{i\omega[n(\omega)-1]l}{c}\right) \quad (3.8)$$

and

$$W(\omega)=\frac{2[n(\omega)-1]}{D(\omega)}\exp\left(\frac{i\omega[3n(\omega)-1]l}{c}\right), \quad (3.9)$$

where

$$D(\omega)=[n(\omega)+1]^2-[n(\omega)-1]^2\exp[4i\omega n(\omega)l/c]. \quad (3.10)$$

The field on the right of the slab is given by

$$\hat{A}^+(x,t)=\int_0^\infty d\omega\left(\frac{\hbar}{4\pi\varepsilon_0 c\omega S}\right)^{1/2}[\hat{b}_R(\omega)e^{i\omega x/c} + \hat{b}_L(\omega)e^{-i\omega x/c}]e^{-i\omega t}, \quad x>l, \quad (3.11)$$

where the operator for the rightwards-propagating outgoing field is given by

$$\hat{b}_R(\omega)=T_S(\omega)\hat{a}_R(\omega)+R_S(\omega)\hat{b}_L(\omega)+\hat{F}_R(\omega), \quad (3.12)$$

similar to I (5.15), and the form of the noise operator on the right is obtained from that on the left, given by Eq. (3.5), according to the prescription

$$\hat{F}_R(\omega)=\hat{F}_L(\omega) \quad \text{with } x'\rightarrow -x' \text{ in the exponents.} \quad (3.13)$$

These outward propagating noise operators differ from those given in I by the occurrence of the modulus of the extinction coefficient in the square-root prefactors and by the generalization of the normalized noise current operator to the form defined in Eq. (2.21).

It is straightforward, but algebraically lengthy, to show with the use of the commutator (2.22) and the forms of the coefficients (3.6)–(3.9) that the noise operators in (3.4) and (3.12) have the commutators

$$[\hat{F}_L(\omega),\hat{F}_L^\dagger(\omega')]=[\hat{F}_R(\omega),\hat{F}_R^\dagger(\omega')] =[1-|R(\omega)|^2-|T(\omega)|^2]\delta(\omega-\omega') \quad (3.14)$$

and

$$[\hat{F}_L(\omega),\hat{F}_R^\dagger(\omega')]=-[R_S(\omega)T_S^*(\omega)+T_S(\omega)R_S^*(\omega)] \times\delta(\omega-\omega'). \quad (3.15)$$

These noise-operator commutators and the forms of the outgoing field operators defined in Eqs. (3.4) and (3.12) have been applied in [18] to derive the field commutation relations in an optical cavity. It follows from the above expressions that the outgoing field operators have the simple free-space commutators

$$[\hat{a}_L(\omega),\hat{a}_L^\dagger(\omega')]=[\hat{b}_R(\omega),\hat{b}_R^\dagger(\omega')]=\delta(\omega-\omega') \quad (3.16)$$

and

$$[\hat{a}_L(\omega),\hat{b}_R^\dagger(\omega')]=0. \quad (3.17)$$

Expressions for the electric- and magnetic-field operators on the left and right of the slab are readily obtained from Eqs. (3.3) and (3.11), respectively, with the use of Eq. (2.8).

B. Interior region

The vector potential operator inside the dielectric slab has the form

$$\hat{A}^+(x,t)=\int_0^\infty d\omega\left(\frac{\hbar\eta(\omega)}{4\pi\varepsilon_0 c\omega n(\omega)^2 S}\right)^{1/2}[\hat{c}_R(x,\omega) + \hat{c}_L(x,\omega)]e^{-i\omega t}, \quad -l<x<l, \quad (3.18)$$

where the operators associated with the rightward- and leftward-propagating fields are again linear combinations of the incoming field operators and noise contributions, with the forms

$$\hat{c}_R(x,\omega)=\left(\frac{n(\omega)}{\eta(\omega)^{1/2}}[V(\omega)\hat{a}_R(\omega)+W(\omega)\hat{b}_L(\omega)] +i\left(\frac{2\omega|\kappa(\omega)|}{c}\right)^{1/2} \times\left\{\int_{-l}^{l}dx'\left[\frac{n(\omega)^2-1}{D(\omega)}\exp\left(\frac{i\omega n(\omega)(2l+x')}{c}\right) +\frac{[n(\omega)-1]^2}{D(\omega)}\exp\left(\frac{i\omega n(\omega)(4l-x')}{c}\right)\right]\hat{\varphi}(x',\omega) +\int_{-l}^{x}dx'\exp\left(-\frac{i\omega n(\omega)x'}{c}\right)\hat{\varphi}(x',\omega)\right\}\right) \times\exp\left(\frac{i\omega n(\omega)x}{c}\right) \quad (3.19)$$

and

$$\hat{c}_L(x,\omega)=\left(\frac{n(\omega)}{\eta(\omega)^{1/2}}[W(\omega)\hat{a}_R(\omega)+V(\omega)\hat{b}_L(\omega)] +i\left(\frac{2\omega|\kappa(\omega)|}{c}\right)^{1/2} \times\left\{\int_{-l}^{l}dx'\left[\frac{n(\omega)^2-1}{D(\omega)}\exp\left(\frac{i\omega n(\omega)(2l-x')}{c}\right) +\frac{[n(\omega)-1]^2}{D(\omega)}\exp\left(\frac{i\omega n(\omega)(4l+x')}{c}\right)\right]\hat{\varphi}(x',\omega) +\int_{x}^{l}dx'\exp\left(\frac{i\omega n(\omega)x'}{c}\right)\hat{\varphi}(x',\omega)\right\}\right) \times\exp\left(-\frac{i\omega n(\omega)x}{c}\right), \quad (3.20)$$

similar to I (5.17) and (5.18). The commutation relations for these operators are the same as given in the Appendix of I,

and there is no need to reproduce them here. Their equations of propagation are easily derived from Eqs. (3.19) and (3.20) as

$$\frac{\partial \hat{c}_{R,L}(x,\omega)}{\partial x} = \pm i \frac{\omega n(\omega)}{c} \hat{c}_{R,L}(x,\omega) \pm i \left(\frac{2\omega|\kappa(\omega)|}{c} \right)^{1/2} \hat{\varphi}(x,\omega), \quad (3.21)$$

where + and − refer to right and left propagation, respectively. The electric- and magnetic-field operators inside the slab are straightforwardly derived from Eq. (2.8) with the use of Eqs. (3.18) and (3.21). It has been shown in [6] that the same expressions for the vector potential operator as derived in the present section can be obtained by taking the propagation equation (3.21) as the starting point and applying the usual boundary conditions to the field operators at the surfaces of the slab.

All of the field operators in the three spatial regions are expressed in terms of the two incoming fields associated with $\hat{a}_R(\omega)$ and $\hat{b}_L(\omega)$, together with the noise field associated with $\hat{\varphi}(x,\omega)$. The states of the entire system are thus defined by the states of the two incoming optical fields and by the expectation values of the noise operator. For specified inputs, the formalism allows the time development of the optical fields from their initial input states to be calculated.

C. Canonical commutation relation

The correctness of the quantized field operators can be tested by evaluation of the canonical commuator, which should have the value given in Eq. (2.16). The test can be carried out by use of the explicit forms of the field operators, as in [6], or more concisely by use of the expression (2.15), which is determined by the same Green functions as the field operators themselves. The calculations are largely the same as presented for the attenuating dielectric in I, and it is not necessary to repeat most of the detail. However, the possibility that $\kappa(\omega)$ may be negative for some ranges of the frequency ω requires additional consideration of the structures of the poles in the various reflection and transmission coefficients. Thus, while $\varepsilon(\omega)$ continues to have all of its poles in the lower half of the complex ω plane, as outlined in Sec. II, this condition is no longer automatically the case for some of the coefficients that are derived from $\varepsilon(\omega)$.

The reflection coefficient at each surface for light incident from inside the dielectric slab is

$$r(\omega) = \frac{n(\omega)-1}{n(\omega)+1} \equiv |r(\omega)| \exp[i\phi_r(\omega)], \quad (3.22)$$

where the amplitude has the property $|r(\omega)| \leq 1$ for all values of the frequency, whether ω corresponds to dielectric loss or gain. The complex round-trip loss or gain for light that travels from a point in the slab and back to the same point after two surface reflections is

$$g(\omega) = r^2(\omega) \exp[4i\omega n(\omega) l/c] \equiv |g(\omega)| \exp[i\phi_g(\omega)], \quad (3.23)$$

where

$$|g(\omega)| = |r(\omega)|^2 \exp[-4\omega\kappa(\omega) l/c],$$

$$\phi_g(\omega) = 2\phi_r(\omega) + [4\omega\eta(\omega) l/c]. \quad (3.24)$$

The denominator (3.10) that occurs in the coefficients defined in Eqs. (3.6)–(3.9) can be written in the form

$$D(\omega) = [n(\omega)+1]^2 [1-g(\omega)]. \quad (3.25)$$

The numerators of these coefficients and the denominator (3.25) are analytic functions of ω in the upper half of the complex ω plane and the coefficients are themselves analytic functions if $1-g(\omega)$ has no zeros there. The zeros of $1-g(\omega)$ occur for frequencies ω that simultaneously satisfy

$$|g(\omega)| = 1 \quad (3.26)$$

and

$$\cos[\phi_g(\omega)] = 1. \quad (3.27)$$

The function $g(\omega)$ is also analytic in the upper half plane and $|g(\omega)|$ accordingly takes its maximum value on the boundary of the half plane [19]. Now $|g(\omega)|$ clearly tends to zero on the infinite semicircle, so that its maximum value must occur on the real axis. A sufficient condition for analytic coefficients is therefore

$$|g(\omega)| < 1 \quad \text{for real} \quad \omega, \quad (3.28)$$

and this is always satisfied for frequencies associated with loss, where $\kappa(\omega)$ is positive. However, for frequencies associated with gain, where $\kappa(\omega)$ is negative, the condition (3.28) is satisfied only for

$$|r(\omega)| < \exp[-2\omega|\kappa(\omega)| l/c]. \quad (3.29)$$

In this case the coefficients are indeed analytic functions of ω in the upper half plane, and the proofs of the canonical commutation relation (2.16) for the different regions of space proceed in exactly the same ways as presented in I for the purely attenuating dielectric. These proofs justify the normalization of the noise commutator assumed in Eq. (2.17).

The conditions (3.26) and (3.27) determine the threshold for laser action, when the state of the optical field in the amplifying slab transforms into one of self-sustaining oscillation. The two conditions must be satisfied simultaneously for the lasing frequencies ω. Condition (3.26) specifies a gain in the dielectric that is sufficient to offset the loss of optical energy through the slab surfaces while condition (3.27) specifies phase matching of the light after a round trip in the slab. We do not consider the properties of the lasing slab here.

IV. SLAB AMPLIFICATION OR ATTENUATION AND NOISE

The slab acts as an amplifier or attenuator for radiation incident from the free space on its left or right. The system must also produce noise in amounts whose minimum values are controlled by very general requirements derived from the relations between input and output operators [20]. We show in the present section how the gain and the noise derived from the slab properties obtained above conform to these

requirements. We also evaluate the electric-field fluctuations in the three spatial regions.

A. Gain and noise

The slab geometry shown in Fig. 1 is symmetrical, and we need consider only its effects on light that is incident from the free space on its left, with the incident field from the right taken to be in its vacuum state. Thus, with the use of Eqs. (3.4) and (3.12), the output photon-number fluxes on the left and right of the slab are determined by the expectation values

$$\langle \hat{a}_L^\dagger(\omega)\hat{a}_L(\omega')\rangle = G_R(\omega)\langle \hat{a}_R^\dagger(\omega)\hat{a}_R(\omega')\rangle + \langle \hat{F}_L^\dagger(\omega)\hat{F}_L(\omega')\rangle \tag{4.1}$$

and

$$\langle \hat{b}_R^\dagger(\omega)\hat{b}_R(\omega')\rangle = G_T(\omega)\langle \hat{a}_R^\dagger(\omega)\hat{a}_R(\omega')\rangle + \langle \hat{F}_R^\dagger(\omega)\hat{F}_R(\omega')\rangle. \tag{4.2}$$

The intensity gains in reflection and transmission are defined by

$$G_R(\omega) = |R_S(\omega)|^2 \tag{4.3}$$

and

$$G_T(\omega) = |T_S(\omega)|^2, \tag{4.4}$$

respectively, where the reflection and transmission coefficients are given by Eqs. (3.6) and (3.7). We use the term ''gain'' for simplicity to cover both amplifying and attenuating frequencies, when the $G(\omega)$ are greater or smaller than unity, respectively. These gains have the properties

$$\begin{aligned} G_R(\omega)+G_T(\omega) &> 1 \quad \text{for} \quad \kappa(\omega) < 0 \\ &= 1 \quad \text{for} \quad \kappa(\omega) = 0 \\ &< 1 \quad \text{for} \quad \kappa(\omega) > 0. \end{aligned} \tag{4.5}$$

Both the reflection and transmission coefficients have the denominator $D(\omega)$, which can be written in the form (3.25), and they therefore have the proportionality

$$G(\omega) \propto \frac{1}{|1-g(\omega)|^2} = \frac{1}{1+|g(\omega)|^2-2|g(\omega)|\cos[\phi_g(\omega)]}, \tag{4.6}$$

where Eq. (3.23) has been used. The gains have their maximum values for $\cos[\phi_g(\omega)]=1$ when

$$G_{\max}(\omega) \propto \frac{1}{[1-|g(\omega)|]^2} \tag{4.7}$$

and infinite gain occurs for $|g(\omega)|=1$, corresponding to the threshold for laser action discussed in Sec. III C. The gain remains finite for $|g(\omega)|<1$ and Eq. (4.6) takes half its maximum value (4.7) when

$$\cos[\phi_g(\omega)] = 1 - \frac{[1-|g(\omega)|]^2}{2|g(\omega)|}. \tag{4.8}$$

Thus, as the round-trip gain $|g(\omega)|$ approaches the threshold value of unity, $\phi_g(\omega)$ at half maximum gain differs from its value at maximum gain (an integer multiple of 2π) by approximately $\pm[1-|g(\omega)|]$. The full width of the gain profile at half maximum height close to threshold is now obtained from the second line of Eq. (3.24) as

$$\Delta\omega = \frac{c[1-|g(\omega)|]}{2\eta(\omega)l}. \tag{4.9}$$

The divergence in peak gain (4.7) and the narrowing of the gain profile shown by Eq. (4.9) on the approach to threshold are well-known features of standard laser theory [21].

The output noise operator expectation values that occur in Eqs. (4.1) and (4.2) are readily obtained from essentially the same calculation that produces the commutation relations (3.14), with the help of the corresponding expectation values for the noise current operator given in Eqs. (2.28) and (2.29). The results can be written in the forms

$$\begin{aligned} \langle \hat{F}_L^\dagger(\omega)\hat{F}_L(\omega')\rangle &= \langle \hat{F}_R^\dagger(\omega)\hat{F}_R(\omega')\rangle \\ &= \begin{bmatrix} N(\omega,|T|)+1 \\ -N(\omega,T) \end{bmatrix} \\ &\quad \times \{G_R(\omega)+G_T(\omega)-1\}\delta(\omega-\omega') \end{aligned} \tag{4.10}$$

and

$$\begin{aligned} \langle \hat{F}_L(\omega)\hat{F}_L^\dagger(\omega')\rangle &= \langle \hat{F}_R(\omega)\hat{F}_R^\dagger(\omega')\rangle \\ &= \begin{bmatrix} N(\omega,|T|) \\ -N(\omega,T)-1 \end{bmatrix} \\ &\quad \times \{G_R(\omega)+G_T(\omega)-1\}\delta(\omega-\omega'), \end{aligned} \tag{4.11}$$

where here, and subsequently, the upper and lower entries in the column matrix refer to frequencies for which the dielectric is amplifying and attenuating, respectively. These expectation values are always positive or zero in accordance with the inequalities in Eq. (4.5). The subtraction of Eq. (4.10) from Eq. (4.11) produces expressions consistent with the commutator (3.14) for both cases of amplification and attenuation.

The dielectric slab considered here is an example of a phase-insensitive linear amplifier, whose output noise operators must satisfy the requirements of general amplification theory [20]. The theory needs some extensions to cover the kind of amplifier considered here, in which there are two inputs and two outputs [22], and the generalizations of Eqs. (4.19b) and (4.21) of [20] give

$$\begin{aligned} &\langle \hat{F}(\omega)\hat{F}^\dagger(\omega') + \hat{F}^\dagger(\omega')\hat{F}(\omega)\rangle \\ &\quad \geqslant |G_R(\omega)+G_T(\omega)-1|\,\delta(\omega-\omega'), \end{aligned} \tag{4.12}$$

which must be satisfied by the noise operators on both the left and right of the slab. We note from Eq. (4.5) that the modulus signs in Eq. (4.12) have no effect for $\kappa(\omega)<0$, but they reverse the signs of the terms within for $\kappa(\omega)>0$. Use

of the explicit noise operator expectation values for the amplifying or attenuating slab obtained from Eqs. (4.10) and (4.11) gives

$$\begin{aligned}&\langle \hat{F}_L(\omega)\hat{F}_L^\dagger(\omega')+\hat{F}_L^\dagger(\omega')\hat{F}_L(\omega)\rangle\\&\quad=\langle \hat{F}_R(\omega)\hat{F}_R^\dagger(\omega')+F_R^\dagger(\omega')\hat{F}_R(\omega)\rangle\\&\quad=\begin{bmatrix}2N(\omega,|T|)+1\\-2N(\omega,T)-1\end{bmatrix}\{G_R(\omega)+G_T(\omega)-1\}\delta(\omega-\omega'),\end{aligned}\tag{4.13}$$

and the positive or zero values of the population factors $N(\omega,T)$ and $N(\omega,|T|)$ ensure that the inequality in Eq. (4.12) is indeed satisfied.

B. Electric-field fluctuations

The noise properties of the system are also manifested by the electric-field fluctuation spectrum in the absence of any input signal, which determines the contributions of the waves that propagate perpendicular to the slab to such properties as atomic spontaneous emission rates and Casimir forces. The power spectrum $S(x,\omega)$ of the electric field fluctuations at position x is defined by

$$\langle \hat{E}(x,\omega)\hat{E}(x,\omega')\rangle = S(x,\omega)\,\delta(\omega-\omega'),\tag{4.14}$$

where the angular brackets denote an expectation value with respect to the vacuum states of the incoming fields described by the operators $\hat{a}_R(\omega)$ and $\hat{b}_L(\omega)$ and the positive- or negative-temperature thermal states of the noise field in the amplifying or attenuating slab.

We have previously used the fluctuation-dissipation theorem to obtain expressions for the power spectra associated with various configurations of attenuating dielectrics at zero temperature [1,2,5]. Fluctuation-dissipation theorems have also been derived for amplifying media [23–25]. However, this approach cannot be used when the system as a whole is not in thermal equilibrium [26], as in the present example where an attenuating or amplifying dielectric at elevated positive or negative temperature is surrounded by free space at zero temperature.

The required power spectra can, however, be derived by direct substitution of the electric-field operators in the definition (4.14). Consider first the free space on the right of the slab where the electric field operator obtained from Eqs. (2.8), (3.11), and (3.12) is

$$\begin{aligned}\hat{E}^+(x,\omega)=i\left(\frac{\hbar\omega}{2\varepsilon_0 cS}\right)^{1/2}&\{[T_S(\omega)\hat{a}_R(\omega)+R_S(\omega)\hat{b}_L(\omega)\\&+\hat{F}_R(\omega)]e^{i\omega x/c}+\hat{b}_L(\omega)e^{-i\omega x/c}\}.\end{aligned}\tag{4.15}$$

Substitution in Eq. (4.14) then leads to an exterior spectrum

$$\begin{aligned}S_{\rm ex}(x,\omega)=\frac{\hbar\omega}{\varepsilon_0 cS}\Bigg\{1+\mathrm{Re}[R_S(\omega)e^{2i\omega x/c}]+\begin{bmatrix}N(\omega,|T|)+1\\-N(\omega,T)\end{bmatrix}\\\times[|R_S(\omega)|^2+|T_S(\omega)|^2-1]\Bigg\}\end{aligned}\tag{4.16}$$

for $x>l$, where Eqs. (3.1), (4.3), (4.4), and (4.13) have been used. For a blackbody limit in which both the reflection and transmission coefficients vanish, the exterior spectrum of an absorbing slab reduces to

$$S_{\rm ex}(x,\omega)=\frac{\hbar\omega}{\varepsilon_0 cS}[N(\omega,T)+1].\tag{4.17}$$

Here the thermal factor can be separated into a contribution from $N(\omega,T)$ blackbody photons plus a $\frac{1}{2}$ vacuum part propagating away from the slab and another $\frac{1}{2}$ vacuum contribution propagating towards the slab. The former contribution agrees with the one-dimensional form of the blackbody spectrum [4,17].

The electric-field operator in the interior of the slab is similarly obtained with the use of Eqs. (3.18)–(3.20), and the resulting power spectrum can be written as

$$\begin{aligned}S_{\rm in}(x,\omega)=S_{\rm vac}(x,\omega)+\begin{bmatrix}N(\omega,|T|)+1\\-N(\omega,T)\end{bmatrix}\{&S_{RL}(x,\omega)\\&-2S_{\rm vac}(x,\omega)\}\end{aligned}\tag{4.18}$$

for $-l<x<l$, where

$$\begin{aligned}S_{\rm vac}(x,\omega)=\frac{\hbar\omega}{\varepsilon_0 cS}\frac{1}{|n(\omega)|^2}\mathrm{Re}\Bigg(&n(\omega)\\&+n^*(\omega)[n(\omega)-1]\exp\left(\frac{i\omega[n(\omega)+1]l}{c}\right)\\&\times\Bigg\{W(\omega)+\frac{V(\omega)}{2}\Bigg[\exp\left(\frac{2i\omega n(\omega)x}{c}\right)\\&+\exp\left(-\frac{2i\omega n(\omega)x}{c}\right)\Bigg]\Bigg\}\Bigg)\end{aligned}\tag{4.19}$$

is the power spectrum for an attenuating slab at zero temperature and

$$\begin{aligned}S_{RL}(x,\omega)=\frac{\hbar\omega}{\varepsilon_0 cS}[&|V(\omega)e^{i\omega n(\omega)x/c}+W(\omega)e^{-i\omega n(\omega)x/c}|^2\\&+|W(\omega)e^{i\omega n(\omega)x/c}+V(\omega)e^{-i\omega n(\omega)x/c}|^2]\end{aligned}\tag{4.20}$$

contains the contributions to the spectrum from the incoming modes $\hat{a}_R(\omega)$ and $\hat{b}_L(\omega)$, respectively. For an attenuating slab with incoming modes from free-space regions maintained at the same temperature T as the medium, the power spectrum can be obtained independently from the fluctuation-dissipation theorem in the form

$$S_{\rm in}(x,\omega)=[2N(\omega,T)+1]S_{\rm vac}(x,\omega),\tag{4.21}$$

and the same result follows from Eq. (4.18) when $S_{RL}(x,\omega)$ is neglected. Thus $S_{RL}(x,\omega)$ plays the role of a correction to allow for the fact that the free spaces on both sides of the slab are here assumed at zero temperature, and there are accordingly $N(\omega,T)$ fewer photons incident on the slab from each side.

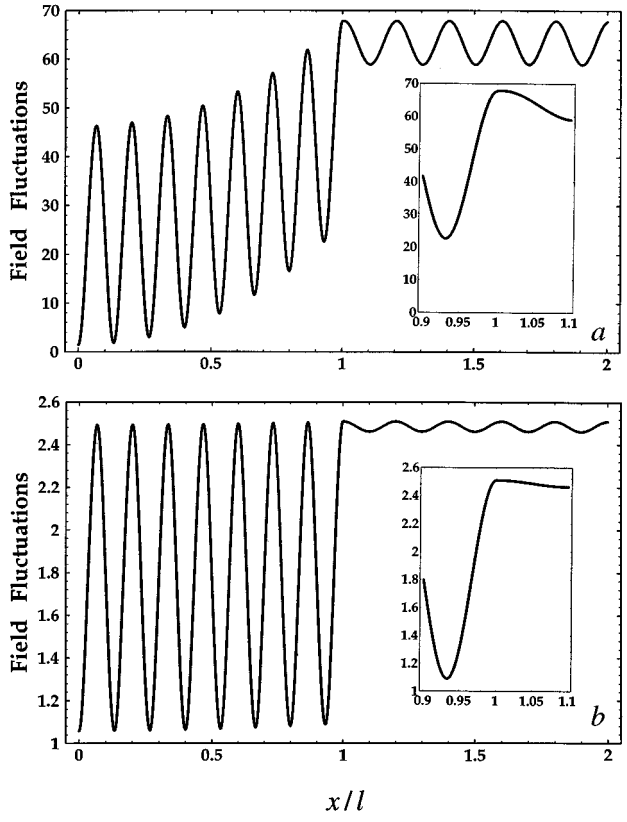

FIG. 2. Spatial variation of the spectrum $S(x,\omega)$ of electric-field fluctuations in the vicinity of an amplifying dielectric slab, normalized to the vacuum free-space value. The slab thickness is $2l=10\pi c/\omega$ and $\eta(\omega)=1.5$. The other parameters are (a) $|T|=0$ and $\kappa(\omega)=-0.04$, giving $G_R(\omega)=19.8$ and $G_T(\omega)=43.5$, and (b) $|T|=180\hbar c/k_B l$ and $\kappa(\omega)=-0.0017$, giving $G_R(\omega)=0.00055$ and $G_T(\omega)=1.12$. The insets show the boundary regions in more detail.

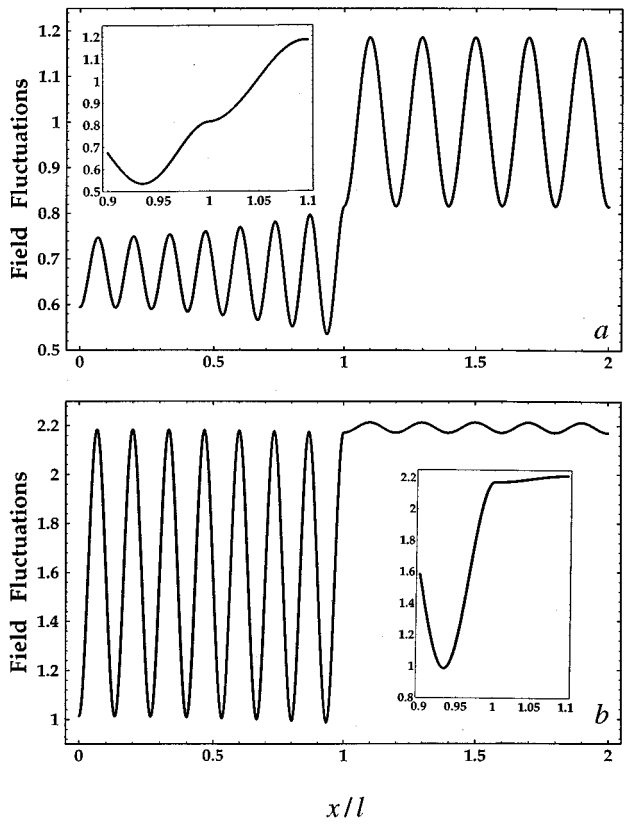

FIG. 3. Spatial variation of the spectrum $S(x,\omega)$ of electric-field fluctuations in the vicinity of an attenuating dielectric slab, normalized to the vacuum free-space value. The slab thickness is $2l=10\pi c/\omega$ and $\eta(\omega)=1.5$. The other parameters are (a) $T=0$ and $\kappa(\omega)=0.04$, giving $G_R(\omega)=0.034$ and $G_T(\omega)=0.075$, and (b) $T=180\hbar c/k_B l$ and $\kappa(\omega)=0.0017$, giving $G_R(\omega)=0.000\,44$ and $G_T(\omega)=0.89$. The insets show the boundary regions in more detail.

The exterior and interior power spectra (4.16) and (4.18) have similar structures with sums of temperature-independent and temperature-dependent terms. It can be shown by lengthy algebra that the former terms have equal values and equal spatial derivatives at $x=l$ while the latter terms have equal values and zero spatial derivatives there. The spectra show maxima at frequencies for which Eq. (3.27) is satisfied, when the round-trip phase shift (3.24) inside the dielectric slab is an integer multiple of 2π, leading to a buildup of the field fluctuations.

Figure 2 shows two examples of the spatial dependences of the power spectrum $S(x,\omega)$ of electric-field fluctuations for a frequency at which amplification occurs. The fluctuations are symmetrical around $x=0$, and only positive values of x are included in the figure. Figure 2(a) shows the spatial dependence for zero effective temperature, where the two-level population is perfectly inverted, while Fig. 2(b) shows the fluctuations for an elevated negative temperature, where the amplification is reduced by the effects of saturation. The population factor that occurs in the dielectric function (2.6) for the two-level model can be written

$$\frac{N_l+N_u}{N_l-N_u}=\begin{bmatrix}-2N(\omega,|T|)-1\\ 2N(\omega,T)+1\end{bmatrix}, \tag{4.22}$$

where the definitions (2.25) and (2.27) have been used for the amplifier and attenuator, respectively. The change in this population factor with an increase in the magnitude of the temperature affects both the refractive index and extinction coefficient. However, for a refractive index that greatly exceeds the extinction coefficient, a change in the population factor mainly influences the extinction coefficient, whose value at elevated negative temperature is assumed to be related to its value $\kappa_0(\omega)$ at zero negative temperature by [17]

$$\kappa(\omega)=\frac{\kappa_0(\omega)}{2N(\omega,|T|)+1}, \tag{4.23}$$

and this relation has been used in the construction of Fig. 2(b). Despite appearances to the contrary, the spectra have continuous values and slopes at $x=l$ as is shown in the large-scale inserts of the boundary region. For the parameter values given in the figure caption, the value of the extinction coefficient at the lasing threshold obtained from Eq. (3.29) is $\kappa(\omega)=-0.051$, so that Fig. 2(a) represents conditions quite close to threshold. Both the internal and external fluctuations are decreased for the conditions of elevated negative temperature and reduced gain shown in Fig. 2(b).

Similar remarks apply to Fig. 3, where the two parts show the spatial dependences of the electric-field fluctuations associated with an attenuating slab at zero and an elevated temperature, the extinction coefficients at the two temperatures being related by (4.23) with the modulus sign removed. Fig. 3(a) is similar to Fig. 3 in I and corresponds to conditions of equilibrium at zero temperature where the fluctuation-dissipation theorem is valid. It shows the effects of the slab in causing oscillations of the mean-square electric field around the usual free-space value in the exterior regions and around a value reduced by the factor $\eta(\omega)/|n(\omega)|^2$ in the interior, as discussed in I. Figure 3(b) shows the enhanced internal fluctuations and reduced external fluctuations at an elevated temperature. The insets again show the continuities of the slopes of the spectra at $x=l$.

It is evident from Figs. 2(b) and 3(b) that similar electric-field fluctuations occur for an amplifier at elevated negative temperature and an attenuator at elevated positive temperature. It can be shown that for frequencies such that $4\omega\eta(\omega)l/c$ is an integer multiple of 2π the spectra (4.16) and (4.18) tend to the common high-temperature forms

$$S_{\rm ex}(x,\omega)=\frac{\hbar\omega}{\varepsilon_0 cS}\left\{1+\frac{\omega|\kappa_0(\omega)|l}{c}\,\frac{\eta(\omega)^2+1}{\eta(\omega)}\right\} \quad (4.24)$$

and

$$S_{\rm in}(x,\omega)=\frac{\hbar\omega}{\varepsilon_0 cS}\,\frac{1}{2\,\eta(\omega)^2}\left\{1+\frac{\omega|\kappa_0(\omega)|l}{c}\,\frac{\eta(\omega)^2+1}{\eta(\omega)}\right\}\times\{\eta(\omega)^2+1+[\eta(\omega)^2-1]\times\cos[2\omega\eta(\omega)x/c]\cos[2\omega\eta(\omega)l/c]\}. \quad (4.25)$$

These expressions are valid as $T\to-\infty$ for the amplifier and as $T\to\infty$ for the attenuator, where the physical states of the medium are identical, with equal populations in the upper and lower levels of the dipole-active transitions.

V. CONCLUSIONS

We have generalized earlier work on the quantization of the electromagnetic field in attenuating dielectrics to cover a dielectric slab that shows amplification over some ranges of frequency. The extinction coefficient $\kappa(\omega)$ is thus allowed to take negative as well as positive values, with a functional form that is limited only by the requirements of causality. We have derived the forms of the electromagnetic field operators inside the slab and in the free-space regions on either side for waves propagated normal to the slab surfaces. The slab approaches a threshold for laser action when $\kappa(\omega)$ takes increasing negative values up to a point where the gain inside the slab overcomes the losses to the outside by transmission through the surfaces. We have identified the presence of laser threshold effects in the quantized field operators, but have confined our treatment to the regime of linear amplification below threshold. The appropriate canonical commutation relations for the conjugate vector potential and electric-field operators in the three spatial regions are satisfied in this regime.

The quantum formalism has been used to derive the amplification and noise properties of the dielectric slab in terms of the intensity gains for a signal incident from free space observed in reflection from or transmission through the slab. The gain profiles show the usual narrowing effects on the approach to the lasing threshold. The amounts of noise added to the amplified, or attenuated, signals have been shown to accord with the minimum values required by a generalization of standard amplifier theory for a slab with two inputs and two outputs. The quantum-mechanical nature of the formalism ensures that it applies to the amplification of nonclassical light, as well as light whose gain characteristics could be obtained from a classical derivation. For any kind of incident light, the added noise is a basic quantum-mechanical phenomenon that can only be rigorously computed by the quantum theory.

Previous work on the quantization of the electromagnetic field in dielectrics has employed models in which the centers of amplification or attenuation are represented by beam splitters, whose input-output relations allow for illumination of the spare input ports with light from harmonic oscillators in inverted or normal states, respectively [15]. This method has been applied to sections of amplifying and attenuating media embedded in inert media of infinite extent [16]. It has also been used in quite sophisticated modeling of spatial and temporal effects in semiconductor lasers in Fabry-Pérot cavities [27]. The results obtained by such models are in qualitative agreement with the more rigorous theory developed here. However, it is difficult to combine the beam-splitter representation with a satisfactory fulfilment of the standard electromagnetic boundary conditions at the surfaces of a finite specimen. By contrast, the formalism presented here can be applied to the study of linear amplification in a finite inverted-population medium, with rigorous inclusion of the spatial effects caused by its surfaces.

The theory developed here is adequate for a wide range of experiments where the light beams are propagated normally through the surfaces of the optical components. Extensions to include all directions of propagation are needed for the treatment of processes such as the spontaneous emission by atoms close to or inside dielectrics and the Casimir pressures exerted on dielectric surfaces, where there is no restriction on the spatial directions involved. Such extensions greatly complicate the derivations, and they are reserved for future work.

ACKNOWLEDGMENTS

We thank Dr. C. R. Gilson, Dr. M. Harris, and Dr. C. H. Henry for helpful discussions. This work was supported by the European Community Human Capital and Mobility Programme through its network on ''Nonclassical Light'' with Contract No. CHRX-CT93-0114. R.M. thanks the University of Kerman Research Council and J.J. thanks the United Kingdom Engineering and Physical Sciences Research Council for financial support.

[1] S. M. Barnett, R. Matloob, and R. Loudon, J. Mod. Opt. **42**, 1165 (1995).
[2] R. Matloob, R. Loudon, S. M. Barnett, and J. Jeffers, Phys. Rev. A **52**, 4823 (1995).
[3] T. Gruner and D.-G. Welsch, Phys. Rev. A **51**, 3246 (1995); **53**, 1818 (1996).
[4] M. Artoni and R. Loudon, Phys. Rev. A **55**, 1347 (1997).
[5] R. Matloob and R. Loudon, Phys. Rev. A **53**, 4567 (1996).
[6] J. Jeffers, S. M. Barnett, R. Loudon, R. Matloob, and M. Artoni, Opt. Commun.. **131**, 66 (1996).
[7] L. D. Landau, E. M. Lifshitz, and L. P. Pitaevskii, *Electrodynamics of Continuous Media*, 2nd ed. (Pergamon, Oxford, 1984), Sec. 82.
[8] M. Altarelli, D. L. Dexter, H. M. Nussenzveig, and D. Y. Smith, Phys. Rev. B **6**, 4502 (1972).
[9] H. M. Nussenzveig, *Causality and Dispersion Relations* (Academic, New York, 1972).
[10] L. W. Davies, Proc. IEEE **51**, 76 (1963).
[11] T. A. Weber and D. B. Trizna, Phys. Rev. **144**, 277 (1966).
[12] R. Y. Chiao, Phys. Rev. A **48**, R34 (1993).
[13] F. Bassani and S. Scandolo, Phys. Rev. B **44**, 8446 (1991).
[14] S. Scandolo and F. Bassani, Phys. Rev. B **45**, 13 257 (1992).
[15] R. J. Glauber, in *Frontiers in Quantum Optics*, edited by E. R. Pike and S. Sarkar (Hilger, Bristol, 1986), p. 534.
[16] J. R. Jeffers, N. Imoto, and R. Loudon, Phys. Rev. **47**, 3346 (1993).
[17] C. H. Henry and R. F. Kazarinov, Rev. Mod. Phys. **68**, 801 (1996).
[18] S. M. Barnett, C. R. Gilson, B. Huttner, and N. Imoto, Phys. Rev. Lett. **77**, 1739 (1996).
[19] Z. Nehari, *Conformal Mapping* (McGraw-Hill, New York, 1952).
[20] C. M. Caves, Phys. Rev. D **26**, 1817 (1982).
[21] A. E. Siegman, *Lasers* (University Science Books, Mill Valley, CA, 1986), pp. 443–451.
[22] S. M. Barnett, A. Gatti, J. Jeffers, and R. Loudon (unpublished).
[23] P. N. Butcher and N. R. Ogg, Proc. Phys. Soc. **86**, 699 (1965).
[24] M.-A. Dupertuis and S. Stenholm, J. Opt. Soc. Am. B **4**, 1094 (1987).
[25] S. Tarzi, J. Phys. A **21**, 3105 (1988).
[26] L. D. Landau and E. M. Lifshitz, *Statistical Physics*, 3rd ed. (Pergamon, Oxford, 1980), Pt. 1, Sec. 123.
[27] D. D. Marcenac and J. E. Carroll, IEE Proc. **140**, 157 (1993).